

Figure S1 (Painter et al)

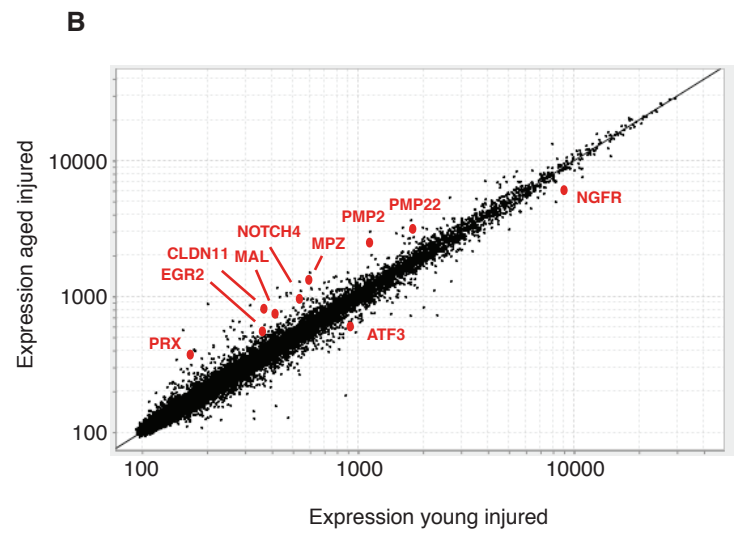
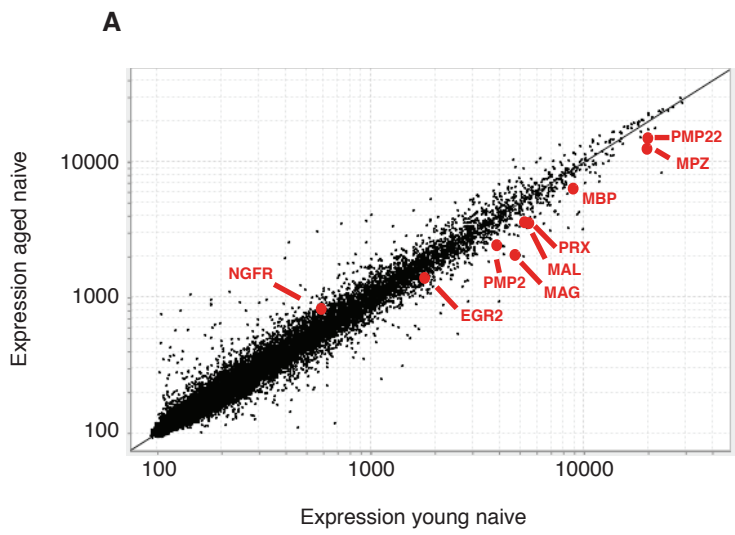
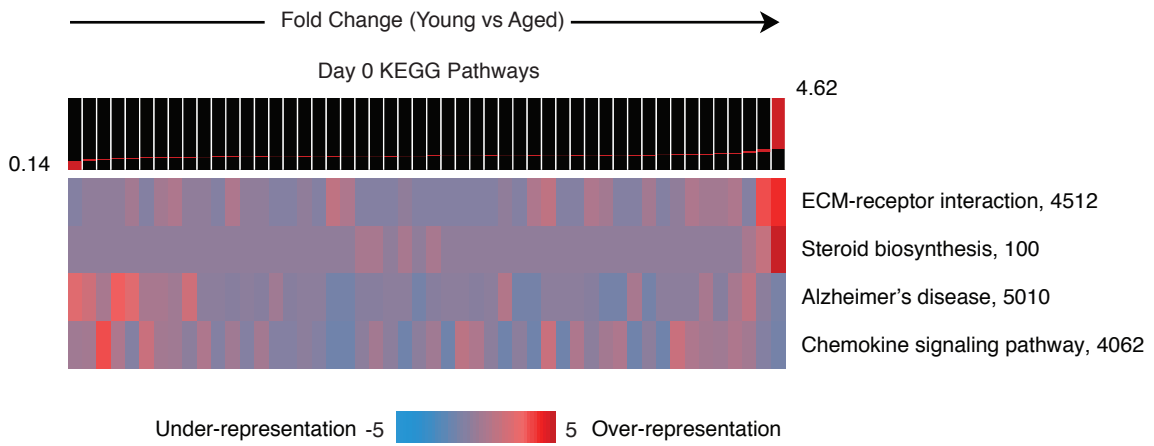


Figure S2 (Painter et al)

A



B

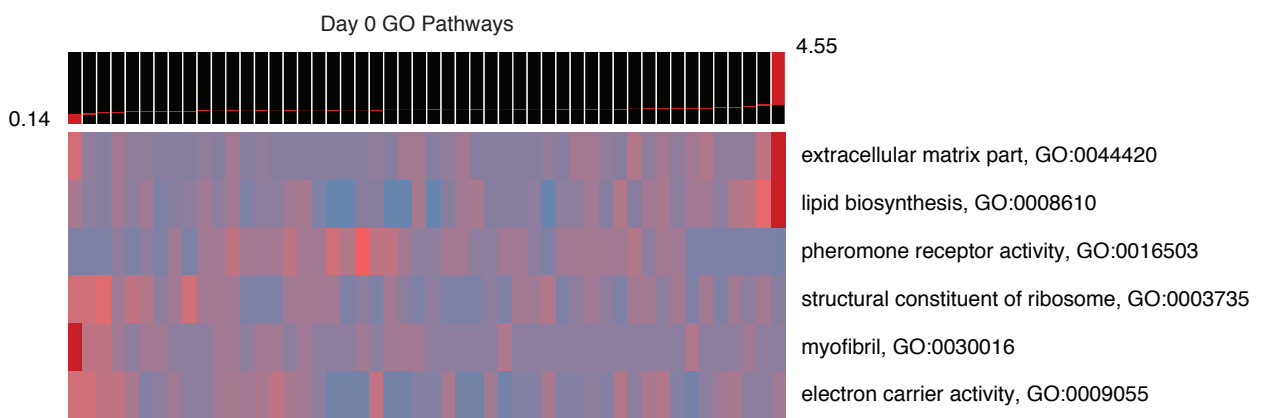


Figure S3 (Painter et al)

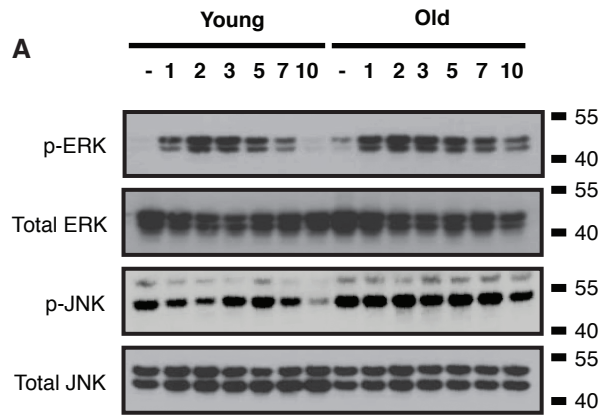


Figure S4 (Painter et al)

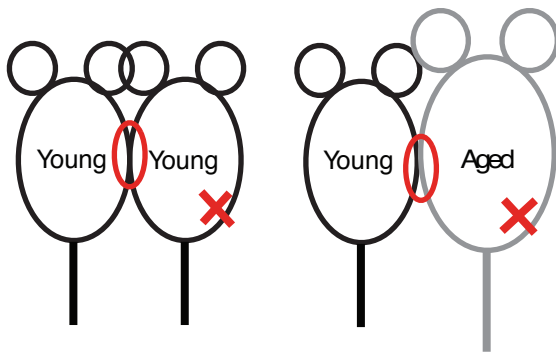
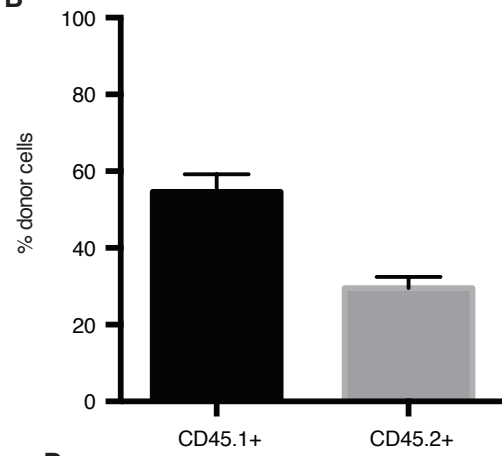
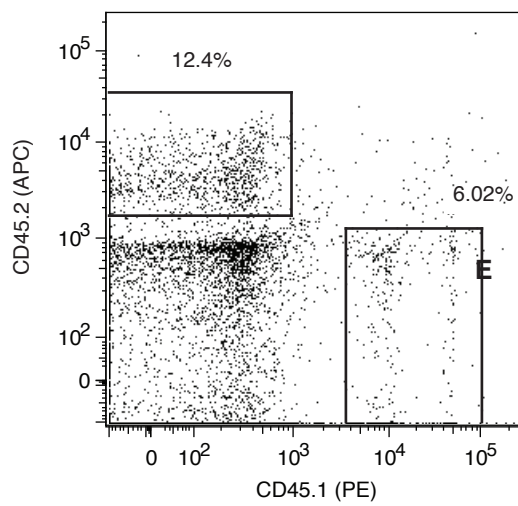
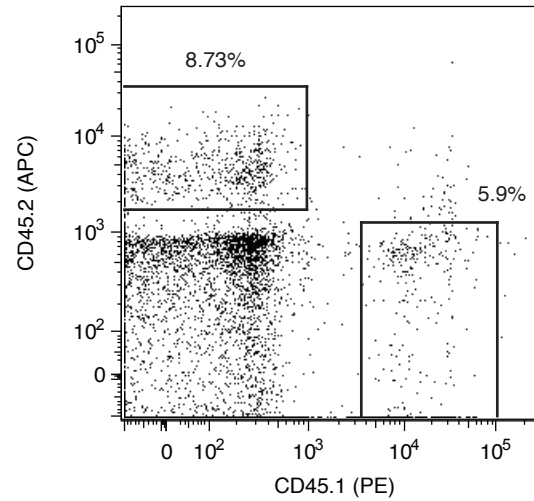
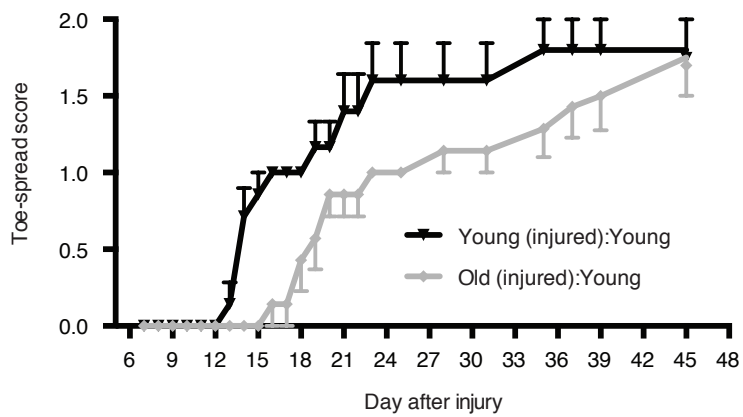
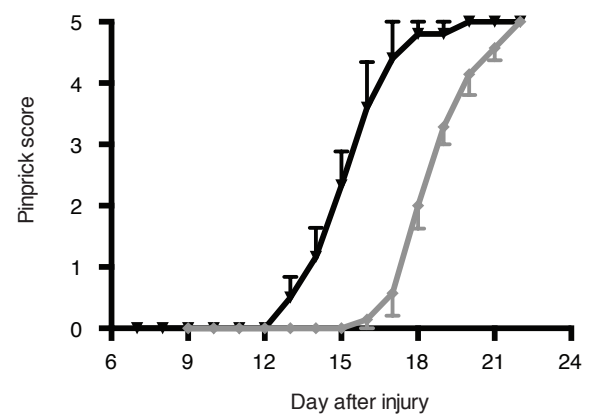
A**B****C****D****E****F**

Figure S5 (Painter et al)

SUPPLEMENTAL MATERIAL

Supplemental Figure Legends

Figure S1, related to Figure 2: Transcriptional profiles of young and aged DRGs are comparable.

Gene-expression data of young and aged DRG neurons. **(A)** Fold Change vs. Fold Change plot. Genes along the black $y=x$ line represent equal Fold Change between naive and injured conditions of either age. Note the vast majority of genes fall roughly along this line. Several genes along the $y=1$ line that are seem to be activated only in young animals represent spurious muscle contamination (MYL1, TNNI2, ATP2A1, TNNC2, ACTA1) with t-test p-values well above 0.4. Red = known regeneration-associated genes. **(B)** Expression vs. expression plot of aged naive vs. aged injured DRGs. Note the injury response is robust. Several known regeneration markers are highlighted in red. Blue lines represent Fold Change = 2, blue numbers in each corner represent the number of genes up or down-regulated by Fold Change of 2.

Figure S2, related to Figure 4: Transcriptional alterations in aged Schwann cells.

(A) Expression vs. expression of naive aged vs. young nerves is plotted. In red, several SC-associated transcripts are highlighted. Note the expression of myelin-related genes is down-regulated in aged animals under steady state conditions. **(B)** Expression vs. expression of injured aged vs. young nerves (day 4 after sciatic nerve crush). Select SC-associated genes are highlighted in red.

Figure S3, related to Figure 4: Gene pathway analyses of young and aged naive nerves.

Significantly over-represented gene pathways from KEGG **(A)** and GO **(B)** databases. Columns represent groups of genes according to their fold change difference in young vs. aged sciatic nerves in naive conditions. The left most column represents genes most over-expressed in old, whereas the right most column represents genes most over-expressed in young. Heat-map depicts the pattern of expression of pathways across these groups of differentially expressed genes (see (Goodarzi et al., 2009)).

Figure S4, related to Figure 4: ERK and JNK regulation unaltered in aged nerves.

(A) Representative Western blot analysis of described proteins at various time-points after sciatic nerve crush injury in young and aged animals.

Figure S5, related to Figure 7: Parabiosis does not affect regeneration in aged animals.

(A) Schematic of parabiosis experiment. Young:young and aged:young pairs were surgically conjoined for thirty days to allow for chimerism and then subjected to sciatic nerve crush. For parabiosis experiments, congenic mouse strains were used (one partner CD45.1+ and one partner CD45.2+). Chimerism of blood cells was thus evaluated by flow cytometry after parabiosis by evaluating the percentage of donor blood within spleens of the host animal **(B)**. Plots are presented as mean \pm SEM, n = 4 mice for each congenic strain. Chimerism of blood cells was also evaluated by flow cytometry in the sciatic nerves of either aged **(C)** or young **(D)** CD45.2+ host animals 7 days after nerve crush injury. Restoration of functional recovery in the injured partner was

assessed through pinprick (**E**) and toe-spreading (**F**) as in **Fig. 1**. Mean \pm SEM, n = 7 per cohort to begin (1 young:young pair died at day 17, another died at day 21, 1 old:young pair died at day 39, 2 others at day 45).

Table S1, related to Figure 2: Differentially expressed DRG genes between young and aged after injury.

Red: genes over-expressed in young greater than 2-Fold. Blue: genes under-expressed in young greater than 2-Fold (less than 0.5).

Table S2, related to Figure 4: Differentially expressed sciatic nerve genes between young and aged under naive conditions. Red: genes over-expressed in young greater than 1.5-Fold; Blue: genes over-expressed in aged greater than 1.5-Fold (less than 0.66).

Table S3, related to Figure 4: Differentially expressed sciatic nerve genes between young and aged after injury. Red: genes over-expressed in young greater than 1.5-Fold; Blue: genes over-expressed in aged greater than 1.5-Fold (less than 0.66).

Experimental Procedures

Mice.

Young (8-12 week old) and aged (24-26 month old) C57/BL6 mice were obtained from Charles River and the National Institute of Aging (NIA), respectively. Thy1 YFP+ animals were bred in house, originally obtained from Jackson Labs, line # 003709. Animals were housed and handled in accordance with protocols approved by the Administrative Panel

on Laboratory Animal Care (APLAC) of Stanford University or in full accordance with the IACUC guidelines of Children's Hospital Boston.

Sciatic nerve crush.

All surgical experiments were performed under 2.5% isoflurane on either young adult mice (8-12 weeks old) or aged mice (24-26 months old). Sciatic nerve crush injury was performed as previously described (Ma et al., 2011). Briefly, the sciatic nerve was exposed at mid-thigh level on the left side of the animal and crushed with smooth forceps for 30 seconds. For experiments involving Schwann cells (Fig 3): Mice were anesthetized using isoflurane. Upper thigh was shaved and sterilized using isopropanol. A 1 cm incision was made using a scalpel and nerve was visualized via blunt dissection using forceps. The left sciatic nerve was crushed at mid-thigh for 5 seconds using forceps marked with sterile graphite to mark the crush site. Carprofen (5mg/kg subcutaneous) was administered for analgesia.

Sciatic nerve graft.

For Thy1 experiments, 1 cm long segments of the sciatic nerve (from mid-thigh level to the site of trifurcation) from either young or aged animals were acutely harvested and grafted using 10-0 nylon sutures onto the sciatic nerve just below the sciatic notch of 8 week old Thy1 YFP mice. These nerves were only sutured at the proximal sight and the distal side was left as a free ending. For nerve graft studies involving behavioral assessments, 3 mm of the sciatic nerve was removed from the host mice and was replaced with a 1cm long sciatic nerve graft of either young or aged animals. The proximal and distal ends were sutured with 10-0 nylon.

Assessment of sensory recovery using a pinprick assay.

Pinprick assay was performed as described previously (Ma et al., 2011). Briefly, mice were habituated on wire mesh cages for 30 minutes, until calm, and then tested for pain responses on the hind paw using a small insect needle. All experiments were repeated by at least 2 separate investigators. In the case of nerve graft studies, experiments were conducted blinded to the age of the donor graft. The person who performed the surgeries never participated in the behavioral experiments.

Assessment of motor recovery by toe-spreading test.

Toe-spreading assay was performed as described previously (Ma et al., 2011). Briefly, mice were gently covered with a piece of cloth and lifted by the tail, uncovering the hind paws for clear observation and the number of toes and extend of toe-spreading was measured for the injured side and compared to the uninjured paw. Again, at least two separate investigators made independent assessments for each experiment. Nerve graft studies were completed blind to age of donor graft and the surgeon did not participate in behavioral studies.

Microarray analysis.

Common pools of RNA were derived from ipsi- (injured) and contralateral (uninjured) L4 and L5 DRGs or ipsi- and contralateral sciatic nerves (1cm long segments distal to the site of injury), amplified, and hybridized to Illumina beadchip arrays. All microarray experiments were conducted in biological triplicates, except for the DRGs from old naive animals, which were done in duplicate. Each replicate was composed of tissue from at least 2 separate animals. All analyses were carried out either in Excel or in GenePattern (www.genepattern.org) using the Multiplot module.

For pathway analyses, fold change differences were calculated between relative expression of each gene in young vs. old mice 0 days and 4 days following injury. iPAGE was then applied on each of these fold change expression profiles to identify pathways that best explain the resulting differences in post-injury gene expression between young and old mice. The following methodology was developed by Goodarzi et al. and is more fully described in (Goodarzi et al., 2009).

The continuous expression profiles were first quantized into 50 discrete equally sized bins. Mutual information was then calculated between the expression profile and the pathway profile, a binary vector with N elements, one for each gene, indicating whether that gene belongs to the given GO or KEGG pathway. A non-parametric randomization statistical test was used to identify significantly informative pathways.

Quantification of neurite outgrowth.

DRG sensory neurons were purified as described previously (Costigan et al., 1998). 1,500-2,000 cells were plated on laminin and fixed 17 hours after plating (for naive) or 12 hours after plating (for pre-conditioned). Quantification was completed using Neuromath as described previously (Ma et al., 2011). Quantification was completed blind to age or condition and repeated three separate times.

Parabiosis.

Parabiotic pairs were joined as previously described (Ruckh et al., 2012). All animals used for parabiotic pairings were male, from congenic strains to avoid immune rejection

between the partners. Parabiotic pairings included isochronic-young pairs (two young mice joined, each 8 weeks old), isochronic-old pairs (two old mice joined, each 24 months old -- all died) and heterochronic pairs (a young mouse joined to an old one, respective ages same as above).

Statistics.

All statistics were completed in GraphPad Prism version 6 for Macintosh with the exception of those in Figure 1, which were completed bioinformatically. A summary of statistics for Figure 1 is here:

The data are classed as ordinal rather than continuous and therefore require non-parametric statistical analysis (transformations were not found to suitably normalize the data). Although there are two factors and the data are repeated, no such overall non-parametric test exists and therefore single factor Kruskal Wallis tests have been performed at pre-determined time points and pairwise Mann Whitney U tests used to determine individual differences between groups relative to the 2 months old group.

Motor toe spread summary.

Kruskal Wallis

Day 11: chi square = 4.2, NS

Day 18: chi square = 5.7, NS

Day 25: chi square = 9.3, $p < 0.01$

Mann whitney 2 vs 12 months: $p < 0.01$, 2 vs 24 months: $p < 0.05$

Day 32: chi square = 7.8, $p < 0.05$

Mann whitney 2 vs 12 months: NS, 2 vs 24 months: $p = 0.01$

Pin prick sensory summary.

Kruskall Wallis

Day 11: chi square = 6.7, $P < 0.05$

Mann whitney = 2 vs 12 months: NS, 2 vs 24 months: NS

Day 12: chi square = 14.7, $p < 0.01$

Mann whitney = 2 vs 12 months: $p < 0.01$, 2 vs 24 months: $p < 0.01$

Day 13: Chi square = 14.2, $p < 0.01$

Mann whitney = 2 vs 12 months: $p < 0.05$, 2 vs 24 months: $p < 0.01$

Day 14: chi square = 14.9, $p < 0.01$

Mann whitney = 2 vs 12 months: $p < 0.01$, 2 vs 24 months: $p < 0.01$

Day 15: chi square = 15.0, $p < 0.01$

Mann whitney = 2 vs 12 months: $p < 0.01$, 2 vs 24 months: $p < 0.01$

Western Immunoblotting.

Sciatic nerves were dissected from young and old mice at indicated days after sciatic nerve injury. Protein lysates from sciatic nerve were extracted in the presence of a protease cocktail tablet (Roche Diagnostics) using RIPA extraction buffer by homogenizer and cell debris was removed by centrifugation (4°C, 15min). Protein concentrations were determined by using BCA protein assay kit (Pierce). Equivalent amounts of protein were loaded and separated by SDS-PAGE and subsequently transfer to an Immobilon-P PVDF transfer membrane (Millipore). After washing in TBS containing Tween-20, blots were blocked in 5% milk for 1h at room temperature and incubated with rabbit polyclonal antibodies against p-ERK (Cell Signaling, 1:500), total ERK (Sigma, 1:1000), p-JNK (Cell Signaling, 1:500), total JNK (Cell Signaling, 1:500), ATF3 (Santa Cruz, 1:500), total c-Jun (Cell Signaling, 1:500), and a mouse monoclonal antibody

against GAPDH (Chemicon, 1:2000). HRP-conjugated secondary antibody (anti-rabbit, anti-mouse, Pierce, 1:5000), an ECL kit (Pierce) and autoradiography film (Genesee Scientific) were used following the manufacturer's protocol for signal detection.

Immunohistochemistry.

Sciatic nerves were harvested distal to crush by perfusing mice with ice cold PBS followed by cold 4% paraformaldehyde. Nerves were postfixed for 5 hours at 4°C. For myelin staining, epineurium was carefully removed and axon bundles were separated along natural divisions using forceps. 3-4 small (~3mm) segments of these bundles were cut at approximately the location of the nerve trifurcation. Segments were permeabilized in ice-cold methanol for 20 minutes and rinsed 3x10 minutes in blocking buffer (10% normal donkey serum, 1% Triton X-100 in PBS) at room temperature (RT). Nerve bundle staining: Briefly, segments were blocked in blocking buffer overnight at 4°C. Segments were incubated in primary antibodies: goat anti p75 (Neuromics, 1:500), rabbit anti-MBP (DAKO 1:100), diluted in blocking buffer at 4°C for 72 hours with rocking followed by 3x10 minute washes at RT and 6x1 hour washes in blocking buffer at 4°C. Secondary antibodies (donkey anti-goat 488, donkey anti-rabbit 563, donkey anti-rat 633, Invitrogen) were diluted 1:1000 in blocking buffer. Segments were incubated in secondary antibody for 48 hours at 4°C with rocking and rinsed as after primary antibody incubation followed by 3 clearing steps in 25%, 50%, and 75% glycerol, respectively, for 24 hours each at 4°C. Nerve bundles were mounted in glycerol-based Vectashield mounting media with DAPI.

For staining of sciatic nerve cross-sections, post-fixed nerves were cryoprotected by sinking in 30% sucrose overnight. Frozen nerves were cryosectioned into 10- μ m sections. Sections were permeabilized with ice-cold methanol for 10 minutes and

blocked in blocking buffer (10% donkey serum, 0.2% Triton X-100) for 1 hour at RT followed by overnight incubation in primary antibody: goat anti p75 (Neuromics, 1:500), rabbit anti S100 (DAKO, 1:500), rat anti CD68 (AbD serotec 1:1000) at 4°C. Following 3x10 minute PBS rinses at room temperature, slides were incubated overnight in secondary antibodies (Invitrogen, 1:1000) at 4°C, rinsed 3x10 minutes in PBS and mounted with Vectashield plus DAPI.

***In vitro* Schwann cell phagocytosis assay.**

Schwann cells were purified 3 days post sciatic nerve crush from 24 month old and 8 week old mice according to the methods described in (Brosius Lutz, 2014). Cells were plated at equal density into wells of a 96-well plate. The following day, cells in each well were rinsed once with DPBS and fed media supplemented with 5% FCS and (need quantity here - doing BCA now) pH sensitive dye (pHRODO) -labeled crude PNS myelin purified according to (Larocca and Norton, 2006). After 2 hours incubation at 37 degrees, cells were trypsinized and resuspended in 30% FCS on ice. For flow cytometry analysis, data was collected in the Stanford Shared FACS Facility obtained using NIH S10 Shared Instrument Grant. Approximately 500 Schwann cells were analyzed per well using the facility's LSRII.UV. Schwann cells to analyze were identified by forwards scatter, side scatter, and viability (DAPI) gating. Mean PE-TR fluorescence (pHRODO) was calculated for each cell population.

Plastic embedding and light microscopic analysis of sciatic nerves.

At 3 and 10 days after sciatic nerve crush injury, mice were intravascularly perfused with a solution containing 2% paraformaldehyde and 2% glutaraldehyde in PBS. The ipsilateral sciatic nerve was dissected out and kept in the fixative solution for 4 hours

and next transferred to PBS. A 5-8 mm tissue segment distal to the crush injury site was removed from the sciatic nerve and immersed in a 1% osmium tetroxide solution (Ted Pella), dehydrated in a graded series of ethanol, and embedded in Epon resin (Ted Pella). Transverse sections at 0.5 μm thickness were stained with Toluidine Blue and cover-slipped on glass slides and viewed in a Nikon E600 light microscope. For each nerve, the number of fibers showing myelin sheath preservation was determined.

Electron microscopy of sciatic nerves.

Ultrathin sections (60-70 nm thickness) were cut from plastic embedded sciatic nerve segments using an RMC Products PowerTome ultramicrotome (Boeckeler Instruments). The ultrathin sections were collected on formvar-coated copper one-hole grids. The sections were counterstained with uranyl acetate and lead citrate and examined using a JEOL 100CX transmission electron microscope.

Quantification.

Quantification was performed using National Institutes of Health Image J. Images were acquired using Zeiss Axio Imager M1 and Axiovision software. Images were analyzed blind.

Internalized myelin quantification: Image of nerve bundle was cropped to uniform size and MBP signal threshold was adjusted to reveal areas of intense MBP accumulation. . Area occupied by MBP/area of nerve in cropped image was determined.

P75/S100 quantification: For each cross-section, S100 and p75 signal threshold was adjusted to exclude background signal. A region of interest (ROI) was created based on the S100 positive area of the cross section. This ROI was applied to the p75 image and the percent of the ROI pixels positive for p75 was determined.

Thy1 YFP+ fibers quantification: Images of nerve sections from each distance from the suture site were taken at 10x magnification (at least 3 separate nerve images per animal per distance). The images were imported into ImageJ, converted to black and white, converted into a binary image, and the number of "masks" was counted for each image. This was done in exactly the same procedure for each image, and all images were taken with the same exposure time.

Confocal images were obtained using a Zeiss LSM510 Meta inverted confocal microscope through the Stanford Neuroscience Microscopy Service, supported by NIH NS069375.